Journal of Physics: Conference Series **181** (2009) 012079 doi:10.1088/1742-6596/181/1/012079

Capturing higher modes of vibration of micromachined resonators

Venkatesh K P and Rudra Pratap

CranesSci MEMS Lab, Department of Mechanical Engineering,Indian Institute of Science, Bangalore, India.

E-mail: pratap@mecheng.iisc.ernet.in

Abstract. MEMS resonators have potential applications in the areas of RF-MEMS, clock oscillators, ultrasound transducers, etc. The important characteristics of a resonator are its resonant frequency and Q-factor (a measure of damping). Usually large damping in macro structures makes it difficult to excite and measure their higher modes. In contrast, MEMS resonators seem amenable to excitation in higher modes. In this paper, 28 modes of vibration of an electrothermal actuator are experimentally captured— perhaps the highest number of modes experimentally captured so far. We verify these modes with FEM simulations and report that all the measured frequencies are within 5% of theoretically predicted values.

1. Introduction

Micromachined resonators have potential applications in RF-MEMS, clock oscillators, resonant sensors such as biological mass detector, optical communications, displays, barcode readers and biomedical imaging [1, 2]. To use these resonators effectively, one needs to find a suitable actuation mechanism that is compatible with MEMS technology. Several actuation schemes are explored by different research groups across the world. They can be classified into electrostatic, piezoelectric, electromagnetic and electrothermal types [3, 4]. The response of the resonator to any actuation mechanism depends on two important characterstics of the resonator — its resonant frequency and quality factor (Q) [5]. Its an easy task to estimate the resonant frequencies using numerical tools but it is challenging to capture the higher modes of vibration of the resonator experimentally [6] as the amplitude of vibration reduces enormously at higher modes.

A resonator can be used in variety of applications depending on the mode shape and resonant frequency. For example an electrothermal actuator can be used as an accelerometer in the first mode and as a micro mirror in second and third modes [3]. So it is essential to determine the resonant frequencies and mode shapes which dictate the suitability of their application. Many researchers are exploring ways to capture the higher modes of vibration, Polytec researchers [4] have reported successful extraction of data for the first four modes of a MEMS device, while the same group in collaboration with MEMUNITY also reported data till seventh mode for a compressor [7]. In 2006, Liang-chia chen [8] reported data till seventh mode of vibration of an AFM cantilever. Mitchell [9] in early 1998 has reported the data for a macro scale plate (with dimensions 18 in $\times$ 18 in $\times$ $\frac{1}{8}$ in) upto the ninth normal mode. Martarelli [10] was successful in capturing the frequencies till 23$^{\text{rd}}$ mode of vibration of turbine blade using Laser Surface

Velocimeter. To the best of our knowledge this is the maximum number of modes captured and reported in the literature till now in the history of structural vibrations.

The current study is partly motivated by a need to explore higher modes of vibration in MEMS devices for sensing purposes. For high Q materials like silicon, most of the damping in oscillations of these devices comes from squeeze film effects [11, 12, 13]. It has been shown that it is possible to reduce this kind of damping and increase the Q of the MEMS resonators by exciting them in higher modes [1]. Of course, the study of higher modes of oscillation is an important area in its own right. What is interesting here is that because of the small scale of the vibrating structure, we are able to capture fairly high modes of oscillation relatively easily. In our experiments we have been able to capture up to 28 modes of out-of-plane vibrations of a resonator from the response to a single excitation. Subsequent numerical simulations have confirmed that the captured modes are indeed what is expected and the measured frequencies are very close to the theoretically predicted values.

In this study we use a MEMS resonator fabricated by SOI MUMPs process [14]. This resonator is actually an electrothermal actuator. Structure of the fabricated device is shown in Figure 1. The structure consists of a proof mass suspended by a set of meandering beams. The beam segments that span the meander width are called span beams, while those connecting the span beams are called connector beams [15]. The meanders are connected to the substrate by means of a set of straight beams. Table 1 provides the details of geometric and material properties of the structure used in simulations. Details of experiments and numerical simulations carried out are provided in the second section.

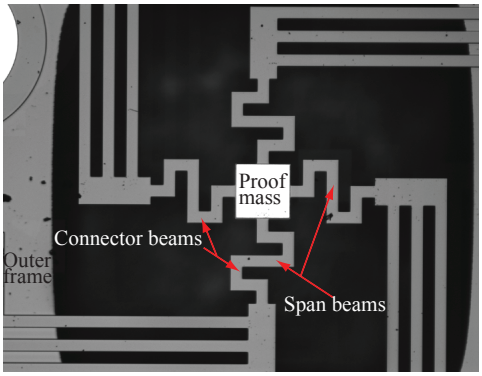

Figure 1. SEM image of the micromachined electrothermal actuator.

Table 1. Mechanical and physical parameters of the electrothermal actuator.

Parameter	Value
Length of straight beams connecting to the substrate, L	1000 μm
Width of straight beams connecting to the substrate, w	45 μm
Thickness of structure, t	25 μm
Length of span beams, l_s	200 μm
Length of connector beams, l_c	100 μm
Proof mass size	200×200 μm^2
Young's modulus, E	130 GPa
Poisson ratio, ν	0.22
Density, ρ	2300 kg/m^3
Co-efficient of thermal expansion, α	2.33×10^{-6} /°C

2. Theory

Here, we discuss the governing equations of elastic structural vibration. We also outline the numerical and experimental procedure to calculate the natural frequencies of the resonator.

2.1. Numerical procedure

In this work, the numerical results are obtained by carrying out modal analysis of the structure in finite-element software, ANSYS [16]. The numerical computation of natural frequencies and the mode shapes involves three main steps. In the first step, the geometric modelling is done in MEMS specific design tool, CoventorWare, by specifying the mask data and fabrication steps involved in realizing the structure. The 3D model is imported into ANSYS and the modal analysis is carried out to estimate the eigenvalues and eigenvectors. For this analysis, the structure is meshed with 25000 eight-noded brick elements. The zero-displacement and zero rotation boundary conditions are applied on the substrate. Then, the theory of elastic dynamics is used for determining the natural frequencies and the corresponding mode shapes of an undamped system.

The general governing equation of motion for free vibration can be written as [5]:

$$[M]\{\ddot{w}\} + [K]\{w\} = 0 \tag{1}$$

where $[M]$ is the structural mass matrix and $[K]$ is the stiffness matrix. If the displacement $w(x, y, z)$ is written in terms of n eigenvectors $\phi_i(x, y)$ and the time dependent modal coordinate $q_i(t)$ [17] as

$$w(x, y, t) = \sum_{i=1}^{n} \phi_i(x, y) q_i(t) \tag{2}$$

then the eigenvalues and the corresponding eigenvectors can be calculated from the equilibrium equations:

$$[K]\{\phi_i\} = \omega_i^2 [M]\{\phi_i\} \tag{3}$$

Based on the orthogonal properties of the eigenvectors, we obtain the expressions for resonant frequencies and corresponding mode shapes:

$$\{\phi_i\}^T [K]\{\phi_i\} = \omega_i^2 \{\phi_i\}^T [M]\{\phi_i\}. \tag{4}$$

Let $\{\phi_i\}^T [K]\{\phi_i\} = K_i$ and $\{\phi_i\}^T [M]\{\phi_i\} = M_i$. Then we get

$$\omega_i^2 = \frac{K_i}{M_i} \tag{5}$$

where M_i and K_i are the mass and stiffness of the structure in i^{th} mode corresponding to the eigenvector ϕ_i and the resonant frequency ω_i.

Finally, the natural frequencies and the corresponding mode shapes (shown in Fig. 4) for all out-of-plane modes are extracted in the postprocessing step. The numerical values of frequencies for the first 28 modes are given in Table 2.

2.2. Experimental procedure

Use of a *Laser Doppler Vibrometer* (LDV) [4] is an attractive method for noncontact dynamic displacement measurements with high positional accuracy. LDVs measure out-of-plane velocities by interferometrically measuring the change in frequency and phase of the back scattered laser light reflected from the surface. In the microsystems analyzer (MSA), the laser light is fed through a microscope to reduce the focused spot size of the laser light [4, 18]. This is important since the velocity is averaged over the spot area and the motion of the small features can only be measured with a small spot size [4]. Single point LDVs require multiple measurements for establishing the mode shapes. Since it is not possible to measure input forces directly, one common technique is to use the excitation voltage as a reference [4]. Response measurements can be sequentially taken at several points, and then combined to provide mode shapes [18]. We have used a Scanning Laser Vibrometer for the experiments conducted in this study.

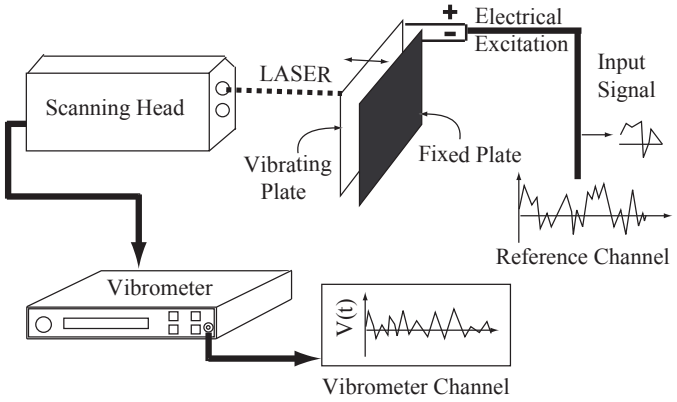

Figure 2. Working principle of the laser doppler vibrometer.

The working principle of the set-up is schematically shown in Fig. 2. The experimentation involves electrical excitation (say $V_{\text{input}} = V_{\text{dc}} + V_{\text{ac}}$, where $V_{\text{ac}} \ll V_{\text{dc}}$) that causes the suspended structure to vibrate. The laser spot from the interferometer in the scanning head is positioned on a scan point on the object by means of mirrors and is scattered back. The back scattered laser light interferes with the reference beam in the scanning head. A photo detector records the interference. A decoder in the vibrometer provides a voltage which is proportional to the velocity of the scanned point parallel to the measurement beam. The voltage is digitized and processed as the vibrometer signal. The output signal can be obtained as velocity or displacement signal using the velocity or the displacement decoder.

The MEMS device under investigation here is an electrothermal actuator. In such devices, hot and cold junctions are generated on application of voltage due to the Peltier effect. Due to thermal expansion, the structure tends to bend. Upon application of a sinusoidal signal, structure starts to vibrate about its equilibrium position. To capture the modal parameters (resonant frequency and damping) of the structure, we apply a pseudorandom signal of voltage 8 ± 2 V during the experimentation. After averaging the FRF of the output signal over 5 times, we determine the resonant frequency of the structure using the frequency response curve, and the corresponding mode shapes are obtained from presentation mode of the vibrometer. Figure 3 shows the frequency response of the structure, natural frequencies and the corresponding mode shapes for the first 28 out-of-plane modes shown in Figure 4.

3. Results and discussion

We now present the results of the numerical and experimental studies. In contrast to such studies at macroscales, we use the experimental results here to validate the numerical results since the finite element model of the structure is likely to have more errors due to uncertainties in material properties and geometric parameters. Figure 3 shows the frequency response of the resonator. From the FRF the modal parameters are extracted and the natural frequencies corresponding to the first 28 modes are as listed in Table 2, and the corresponding mode shapes are shown in

Table 2. Comparison between experimental and numerical results.

Mode No.	f_{exp} (kHz)	f_{num} (kHz)	% error $\lvert\frac{f_{\text{exp}}-f_{\text{num}}}{f_{\text{exp}}}\rvert \times 100$	Mode No.	f_{exp} (kHz)	f_{num} (kHz)	% error $\lvert\frac{f_{\text{exp}}-f_{\text{num}}}{f_{\text{exp}}}\rvert \times 100$
1	32.94	33.97	3.13	15	374.80	377.77	0.79
2	53.75	54.08	0.62	16	395.00	409.64	3.71
3	54.42	54.85	0.79	17	403.30	413.23	2.46
4	73.98	74.14	0.21	18	410.50	413.82	0.81
5	101.80	104.77	2.92	19	424.20	418.26	1.40
6	173.30	174.31	0.58	20	430.20	434.55	1.01
7	183.30	184.44	0.62	21	448.40	445.68	0.61
8	263.90	257.90	2.27	22	482.20	472.75	1.96
9	288.40	296.52	2.81	23	581.60	557.66	4.11
10	295.60	306.24	3.59	24	730.00	731.57	0.21
11	299.50	310.08	3.53	25	740.50	744.76	0.57
12	303.10	314.22	3.67	26	769.40	783.96	1.89
13	324.70	326.12	0.44	27	800.90	791.71	1.14
14	360.20	358.23	0.55	28	878.60	920.52	4.77

Fig. 4. Since the structure is symmetric we can notice many degenerate modes (pseudorepeated modes) [19] such as second and third modes of vibration. Similarly 9$^{\text{th}}$ and 10$^{\text{th}}$, 16, 17, 18 and 19$^{\text{th}}$ modes are again degenerate. The difference between eigenvalues of degenerate modes in

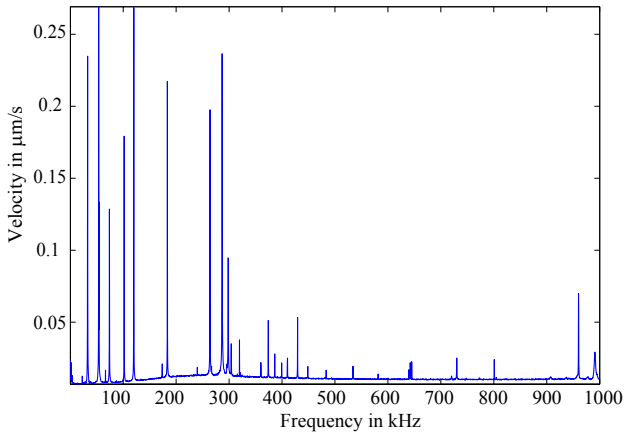

Figure 3. Frequency response function from experimental studies.

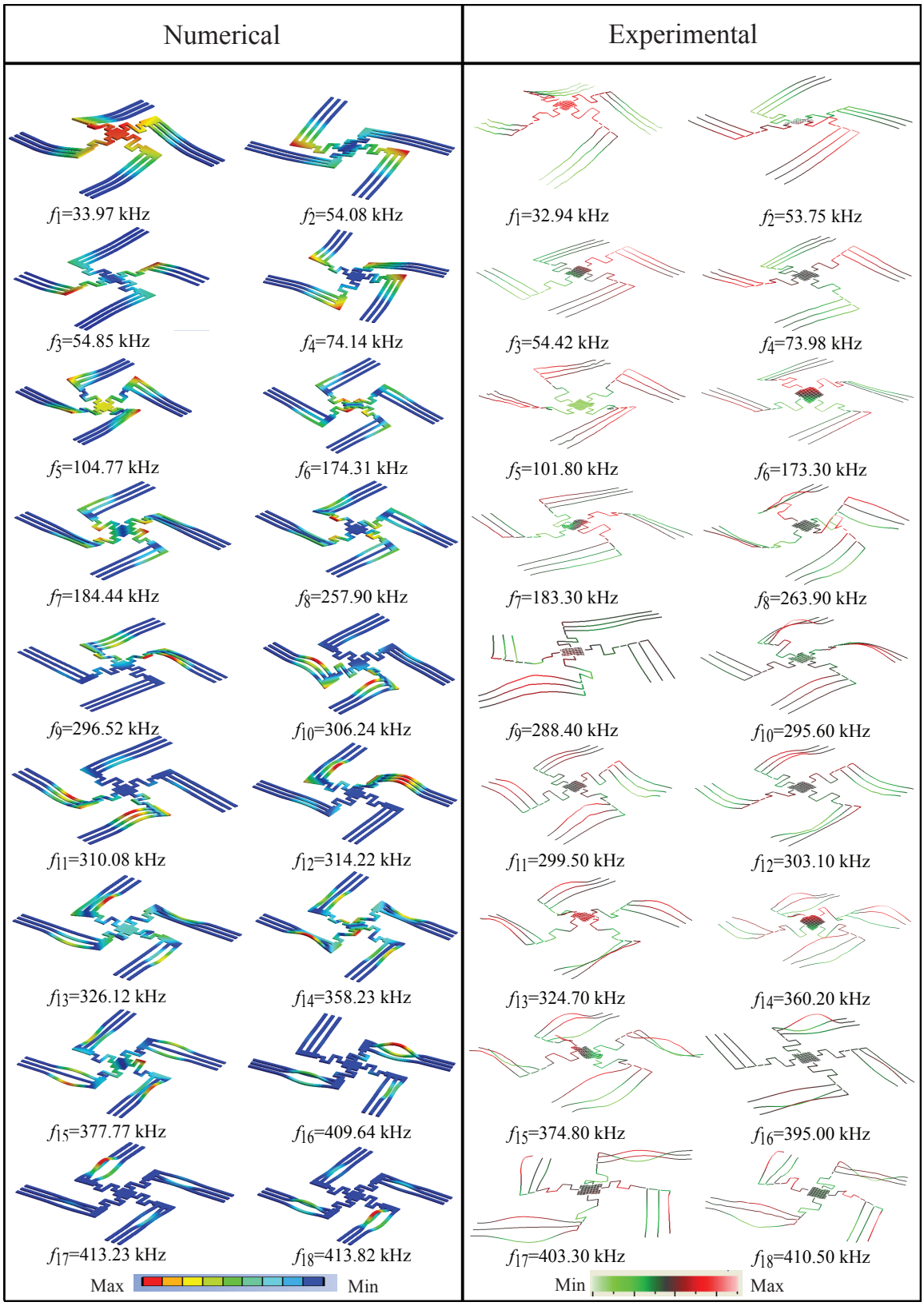
Numerical
Experimental
f_1=33.97 kHz
f_2=54.08 kHz
f_3=54.85 kHz
f_4=74.14 kHz
f_5=104.77 kHz
f_6=174.31 kHz
f_7=184.44 kHz
f_8=257.90 kHz
f_9=296.52 kHz
f_{10}=306.24 kHz
f_{11}=310.08 kHz
f_{12}=314.22 kHz
f_{13}=326.12 kHz
f_{14}=358.23 kHz
f_{15}=377.77 kHz
f_{16}=409.64 kHz
f_{17}=413.23 kHz
f_{18}=413.82 kHz
Max
Min
f_1=32.94 kHz
f_2=53.75 kHz
f_3=54.42 kHz
f_4=73.98 kHz
f_5=101.80 kHz
f_6=173.30 kHz
f_7=183.30 kHz
f_8=263.90 kHz
f_9=288.40 kHz
f_{10}=295.60 kHz
f_{11}=299.50 kHz
f_{12}=303.10 kHz
f_{13}=324.70 kHz
f_{14}=360.20 kHz
f_{15}=374.80 kHz
f_{16}=395.00 kHz
f_{17}=403.30 kHz
f_{18}=410.50 kHz
Min
Max

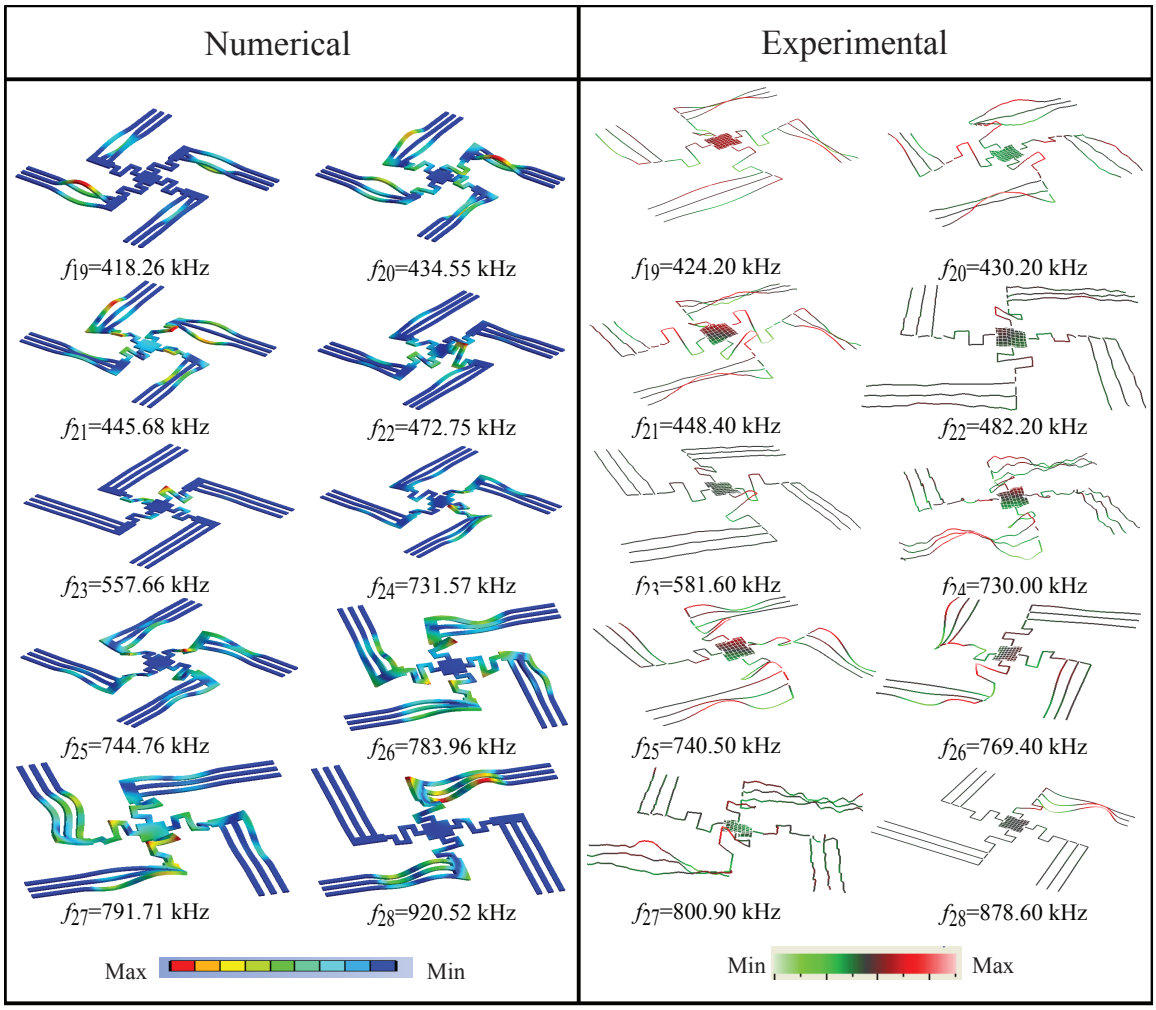

Figure 4. Comparison between numerical and experimental mode shapes.

the symmetric structure indicates of nonuniformities in the modal parameters such as mass and stiffness of the structure [19]. These nonuniformities will further change the dynamic performance characteristics of the system. For example, nonuniformities in mass may result in changes in inertial forces, whereas nonuniformities in stiffness may result in unexpectedly large deflections at certain frequencies in the harmonic response of the system [19]. It can be noticed from Table 2 that numerical and experimental values are very close, with an error less than 5% for all the modes, and the degenerate modes are very close to each other hence reducing the nonuniformities present in the system.

4. Conclusions

We have experimentally determined 28 modes of out-of-plane vibrations of a MEMS resonator. The experimentally measured frequencies are compared with numerically computed values from the modal analysis of the resonator carried out using FEM analysis. The numerically found frequencies match the experimental values within 5% error — can be incredible result especially for higher modes. Our work shows that micro resonators or micro mechanical structures can be excited in fairly higher modes, in contrast to their macro counterparts, rather easily. The

accuracy of results shows that one can confidently employ the higher modes for sensing in MEMS devices. This is particularly significant in the light of the reported results in the literature that Q-factor of a resonator goes up in higher modes if the Q is dominated by squeeze film damping effects.

Acknowledgments
We thank Prof. Navakanta Bhat and Mr. Prasad from Electronics and Communication Engineering Department, IISc., for providing the fabricated structure. This work is supported by a grant from University Grants Commission.

References
[1] A K Pandey and Rudra Pratap 2007 Effect of flexural modes on squeeze film damping in MEMS cantilever resonators *J. Micromech. Microengg.* **17** 2475-2484.
[2] M. Madou 1997 *Fundamentals of Microfabrication* (Florida: CRC Press).
[3] Lijie Li, et.al 2007 Design, simulation and characterization of a MEMS optical scanner *J. Micromech. Microengg.* **17** 1781-1787.
[4] Polytec GmbH– Advanced measurements using light., `http://www.polytec.com`.
[5] S. S. Rao 1995 *Mechanical Vibration* (New York: Wesley Publishing Company).
[6] Chi-Hung Huang and Chien-Ching Ma 2001 Experimental measurement of mode shapes and frequencies for vibration of plates by optical interferometry method *J. Vibrations and acoustics* **276** 276-280.
[7] www.polytec.com/automotive
[8] Liang-chia chen, et.al 2006 High bandwidth dynamic full-field profilometry for nano-scale charecterization of MEMS *J. Physics.* **48** 1058-1062.
[9] L D Mitchell, et.al 1998 An emerging trend in experimental dynamics: merging of laser based three dimensional structural imaging and modal analysis *J. Sound and vibration* **211(3)** 323-333.
[10] M Martarelli, et.al 2001 Automated modal analysis by scanning laser vibrometry: problems and uncertainities associated with the scanning system calibration *J. Mechanical systems and signal processing* **15** 498-508.
[11] R. Pratap, S. S. Mohite and A. K. Pandey 2007 Squeeze-Film Effects in MEMS Devices *J. Indian Institute of Science* **87:1**.
[12] Kwok P. Y., Weinberg M. S. and Breuer K. S 2005 Fluid effects in vibrating micromachined structures. *J. Micromechanical Systems* **14(4)**: 770-781.
[13] Minhang Bao and Heng Yang 2007 Squeeze film air damping in MEMS. *Sensors and Actuators A: Physical* **136**: 327.
[14] SOIMUMPs multi-user MEMS process, MEMSCAP Inc. `http://www.memsrus.com/nc-mumps.soi.html`.
[15] G K. Fedder 1994 *Simulation of micromechanical systems* Doctoral thesis University of California.
[16] ANSYS 10 – *Finite element solver for multiphysics problems.*, `http://www.ansys.com`.
[17] D J Ewins 2000 *Modal Testing: Theory and Practice* (Taunton: Research Studies Press).
[18] Ozdoganlar O Burak, et.al 2005 Experimental modal analysis for microelectromechanical systems *J. Experimental mechanics* **45** 498-506.
[19] Brandon J. Jellison, et.al 2004 Nondestructive evalustion of parts with denerate modes using pseudorepeated roots *J. Dynamic systems, Measurement and control* **126** 498-508.